

# REPORT DOCUMENTATION PAGE

AFRL-SR-BL-TR-01-

Public reporting burden for this collection of information is estimated to average 1 hour per response, including the time for reviewing data needed, and completing and reviewing this collection of information. Send comments regarding this burden estimate or any other aspect of this burden to Department of Defense, Washington Headquarters Services, Directorate for Information Operations and Reports (0704302). Respondents should be aware that notwithstanding any other provision of law, no person shall be subject to any penalty for failing to comply with a collection of information if it does not have a valid OMB control number. PLEASE DO NOT RETURN YOUR FORM TO THE ABOVE ADDRESS.

0022

the  
ng  
ntly

<b>1. REPORT DATE (DD-MM-YYYY)</b> 15-12-2000		<b>2. REPORT TYPE</b> Final Technical Report		<b>3. DATES COVERED (From - To)</b> 01-10-97 - 30-09-00	
<b>4. TITLE AND SUBTITLE</b> Dynamics of Hypervelocity Collisions at the Gas/Surface Interface				<b>5a. CONTRACT NUMBER</b>	
				<b>5b. GRANT NUMBER</b> F49620-98-1-0029	
				<b>5c. PROGRAM ELEMENT NUMBER</b>	
<b>6. AUTHOR(S)</b> Dennis C. Jacobs				<b>5d. PROJECT NUMBER</b>	
				<b>5e. TASK NUMBER</b>	
				<b>5f. WORK UNIT NUMBER</b>	
<b>7. PERFORMING ORGANIZATION NAME(S) AND ADDRESS(ES)</b> University of Notre Dame 511 Main Building Notre Dame, IN 46556				<b>8. PERFORMING ORGANIZATION REPORT NUMBER</b>	
<b>9. SPONSORING / MONITORING AGENCY NAME(S) AND ADDRESS(ES)</b> AFOSR/NL 801 N. Randolph St., Rm. 732 Arlington, VA 22203-1977				<b>10. SPONSOR/MONITOR'S ACRONYM(S)</b> AFOSR/NL	
				<b>11. SPONSOR/MONITOR'S REPORT NUMBER(S)</b>	
<b>12. DISTRIBUTION / AVAILABILITY STATEMENT</b> Approved for public release, distribution unlimited					
<b>13. SUPPLEMENTARY NOTES</b> The views, opinions and/or findings contained in this report are those of the author and should not be construed as an official Air Force position, policy, or decision.					
<b>14. ABSTRACT</b> A series of hyperthermal energy, ion/surface scattering experiments were performed. These studies examined and characterized some of the many processes occurring in energetic gas/surface collisions. In the scattering of Ne <sup>+</sup> on Si(001), the precise amount of momentum, transferred to the surface upon collision, was measured under various conditions. Models that incorporate image charge interactions and inelastic energy loss were successfully applied to simulate the data. The first measurement of atom abstraction at an oxide surface was recorded in the scattering of NO <sup>+</sup> on O/Al(111). Measurement of the product yield and energy distribution as a function of incident energy revealed the detailed reaction mechanism. The growth and erosion of SiO <sub>2</sub> thin films under O <sup>+</sup> bombardment was studied. Isotopic labeling experiments combined with mass-, energy-, and angular-resolved detection provided compelling evidence for a direct Eley-Rideal abstraction of adsorbed oxygen by incident O <sup>+</sup> ions. This reaction pathway competes directly with sputtering channels in the formation of scattered O <sub>2</sub> <sup>-</sup> and SiO <sup>+</sup> . The conclusions from this work help in the modeling of spacecraft interactions with the LEO environment, e.g., vehicle drag, spacecraft charging, oxidation/degradation of exposed surfaces, and the formation of signatures.					
<b>15. SUBJECT TERMS</b> Ion/surface scattering, Energy transfer, satellite drag, abstraction, etching, O <sup>+</sup> , NO <sup>+</sup> , Ne <sup>+</sup> , silicon, silicon oxide, aluminum oxide					
<b>16. SECURITY CLASSIFICATION OF:</b>			<b>17. LIMITATION OF ABSTRACT</b> UL	<b>18. NUMBER OF PAGES</b> 23	<b>19a. NAME OF RESPONSIBLE PERSON</b> Dennis C. Jacobs
<b>a. REPORT</b> Unclassified	<b>b. ABSTRACT</b> Unclassified	<b>c. THIS PAGE</b> Unclassified			<b>19b. TELEPHONE NUMBER (include area code)</b> (219)631-8023

20010116 099

Standard Form 298 (Rev. 8-98)  
Prescribed by ANSI Std. Z39.18

DTIC QUALITY INSPECTED 3

UNIVERSITY OF  
**NOTRE DAME**

Department of Chemistry and Biochemistry  
University of Notre Dame  
Notre Dame, IN 46556

---

Air Force Office of Scientific Research  
Molecular Dynamics Program  
Grant # F49620-98-1-0029  
Final Technical Report  
1 October 1999 – 31 September 2000

**Dynamics of Hypervelocity Collisions at the Gas/Surface Interface**

by  
Dennis C. Jacobs

---

Approved for public release; distribution is unlimited.

---

## Table of Contents

1. EXECUTIVE SUMMARY .....	3
2. INTRODUCTION.....	6
3. EXPERIMENTAL APPROACH.....	6
4. RESULTS AND DISCUSSION.....	10
4.1. ENERGY COUPLING IN HYPERVELOCITY GAS/SURFACE COLLISIONS.....	10
4.2. ATOM ABSTRACTION IN THE SCATTERING OF STATE-SELECTED $\text{NO}^+(\text{X}^1\Sigma^+)$ ON O/AL(111).....	13
4.3. GROWTH AND ETCHING OF SILICON OXIDE THIN FILMS UNDER $\text{O}^+$ BOMBARDMENT .....	16
5. CONCLUSIONS .....	21
6. REFERENCES.....	22

## Table of Figures

FIGURE 1	ATOMIC ION/SURFACE SCATTERING APPARATUS .....	7
FIGURE 2	EXPERIMENTAL APPARATUS FOR SCATTERING STATE-SELECTED MOLECULAR IONS .....	9
FIGURE 3	ANGLE-RESOLVED RELATIVE ENERGY DISTRIBUTION OF 120 eV $\text{Ne}^+$ / Si(001) .....	10
FIGURE 4	COMPARISON OF EMPIRICAL FIT TO $\text{Ne}^+$ /Si(001) SCATTERING DATA.....	12
FIGURE 5	THE COLLISION-ENERGY DEPENDENCE TO $\text{NO}_2^-$ EMERGENCE.....	14
FIGURE 6	VELOCITY DISTRIBUTION OF $\text{NO}_2^-$ PRODUCTS. ....	15
FIGURE 7	YIELD OF $\text{O}_2^-$ VERSUS INCIDENT $\text{O}^+$ ENERGY.....	17
FIGURE 8	MEAN TRANSLATIONAL ENERGY OF SCATTERED $\text{O}_2^-$ PRODUCT .....	18
FIGURE 9	ANGLE-RESOLVED ENERGY DISTRIBUTIONS OF $\text{O}_2^-$ PRODUCTS. ....	19

## 1. Executive Summary

Gas/surface scattering experiments are instrumental in elucidating how an incident particle's energy and approach geometry affect its interaction with a surface target. Three experimental systems were studied to advance our understanding of momentum transfer, charge transfer, and atom transfer in hyperthermal energy, ion/surface collisions. Theoretical models were developed to support and interpret the experimental results.

### Energy Coupling in Hypervelocity Gas/Surface Collisions – $\text{Ne}^+/\text{Si}(001)$

A collimated, monoenergetic (50 – 300 eV) beam of  $\text{Ne}^+$  was targeted at a  $\text{Si}(001)$  surface under ultrahigh vacuum conditions. The scattered ions were collected with angular-, mass-, and energy-resolution. The data are well-described by a model in which the  $\text{Ne}^+$  ion scatters from a single silicon atom on the surface. Inelastic energy losses of 11 eV are consistent with the excitation of surface plasmons.

### Abstraction of O by State-selected Molecular Ions – $\text{NO}^+/\text{O}/\text{Al}(111)$

The first measurement of atom abstraction on an oxide surface was recorded in the scattering of  $\text{NO}^+$  on  $\text{O}/\text{Al}(111)$ . The dependencies of the  $\text{NO}_2^-$  product yield and energy distribution on incident  $\text{NO}^+$  energy are consistent with an Eley-Rideal abstraction mechanism.

### Reaction of $\text{O}^+$ and $\text{O}_2^+$ with an oxidized $\text{Si}(100)$ surface

Isotopic labeling experiments, combined with mass-, energy-, and angular-resolved detection, enable the study of ion/surface reactions under high beam exposures where the surface is significantly modified by the bombarding ions.

Experiments reveal a competition between abstraction and sputtering mechanisms in the emergence of  $O_2^-$  and  $SiO^+$  products. The cross-section for incorporating oxygen ions into the silica film is relatively large, indicating a dynamic exchange of oxygen atoms during hyperthermal energy,  $O^+$  bombardment of  $SiO_2$ .

These state-of-the-art studies have broadened our fundamental understanding of the reaction pathways available to hyperthermal energy, gas/surface collisions. The primary transitions for this research lie in improved modeling of spacecraft drag and erosion of spacecraft materials in low-earth orbit. Technological transfer to the civilian sector is centered around improvements in the fabrication of buried silicon oxide layers and in ion-assisted etching applications employed within the fabrication of microelectronic devices.

Through the support of this AFOSR grant, many students have received invaluable scientific training:

Individual	Position	Current Status
Cecilia Quinteros	Ph.D. student	She will defend her dissertation in Jan., 2000, after which she will work for LAM, Inc. on research in support of microelectronics fabrication
Xiangdong Qin	Ph.D. student	2 <sup>nd</sup> year graduate student continuing on project
Jon Camden	Undergraduate research assist.	After two years of undergraduate research, Jon is now studying for his Ph.D. in physical chemistry at Stanford University.
Stefan Tzanev	Postdoc	Currently working for an optical coatings company
Tochko Tzvetkov	Postdoc	2 <sup>nd</sup> year, continuing on the project.

The research supported through this AFOSR grant has been presented at four international conferences, three national conferences, two regional meetings, and two AFOSR contractors' meetings.

In addition to the four manuscripts currently in preparation, the research findings have been reported in the following publications:

- C. L. Quinteros, T. Tzvetkov, and D. C. Jacobs, (2000) "Eley-Rideal reaction of  $O^+$  with oxidized Si(100)," *Journal of Chemical Physics*, **113**, 5119.
- D. C. Jacobs, "Dynamics of Hypervelocity Gas/Surface Collisions," in *Chemical Dynamics in Extreme Environments*, edited by R. Dressler, *Advanced Series in Physical Chemistry*, World Scientific Publishers, 349 (2000).
- M. Maazouz, T. L. O. Barstis, P. L. Maazouz, and D. C. Jacobs, "Atom abstraction in the Scattering of state-selected  $NO^+(X^1\Sigma^+)$  on O/Al(111)," *Phys. Rev. Lett.* **84**, 1331 (2000).
- M. Maazouz, C. L. Quinteros, T. Tzvetkov, P. L. Maazouz, X. Qin, T. L. O. Barstis, and D. C. Jacobs, "Reactive Collisions of Hyperthermal Ions with Oxide Surfaces" *Proceedings of the Sixteenth International Conference on the Application of Accelerators in Research and Industry: CAARI*, in press (2001).
- C. L. Quinteros, T. Tzvetkov, X. Qin, and D. C. Jacobs "Reactive Scattering of  $O^+$  on oxidized Si(001)" *Nuclear Instruments and Methods in Physics Research B*, in press (2001).

## 2. Introduction

An orbiting space vehicle is continuously exposed to a flux of energetic neutral atoms/molecules, ions, electrons, charged particle radiation, electromagnetic radiation, meteoroids, and orbital debris. This hostile environment can adversely impact the longevity and success of a spacecraft's mission through material degradation, radiation damage, electrostatic charging/arcing, aerodynamic drag, etc.<sup>1</sup> To better understand the dynamics of ion/surface collisions, the processes of energy transfer, charge transfer, and atom abstraction were explored under well-characterized scattering conditions. Detailed mechanisms are presented that can be incorporated into existing models of space vehicle interactions with the low-earth or transfer orbit environments.

## 3. Experimental Approach

An ultrahigh vacuum scattering chamber has been constructed to explore the fundamental processes that occur when hyperthermal energy ions impact surfaces under highly controlled conditions.<sup>2</sup> The apparatus depicted in Fig. 1 consists of four differentially pumped chambers: the source and buffer chambers contain the ion transport optics; the main scattering chamber houses the surface sample and diagnostic tools; and the rotatable detector chamber contains a quadrupole mass spectrometer (QMS). The main chamber is pumped by both a cryopump and an ion pump.

Ions extracted from a Colutron discharge source are accelerated to 1.5 keV, pass through a gas cell for filtering out metastable states, are mass-selected within a Wien filter, and decelerate to the final beam energy (5 – 300 eV). This design delivers up to 100 nA of ion current to the surface in a target area of approximately 1 mm<sup>2</sup>.

The surface sample is heated resistively or by electron bombardment, and the sample mount is cooled by a liquid nitrogen reservoir. A load lock chamber allows

surface samples to be introduced to the main chamber and secured to the manipulator without venting the system. The main scattering chamber is further divided into two sections. The top tier is equipped with routine surface science preparation and analysis tools: low energy electron diffraction (LEED), Auger electron spectroscopy (AES), X-ray photoelectron spectroscopy (XPS), Residual Gas Analyzer (RGA), Kelvin probe for work function measurements, capillary array gas doser, an alkali-atom source, and an ion gun for sputtering the surface clean.

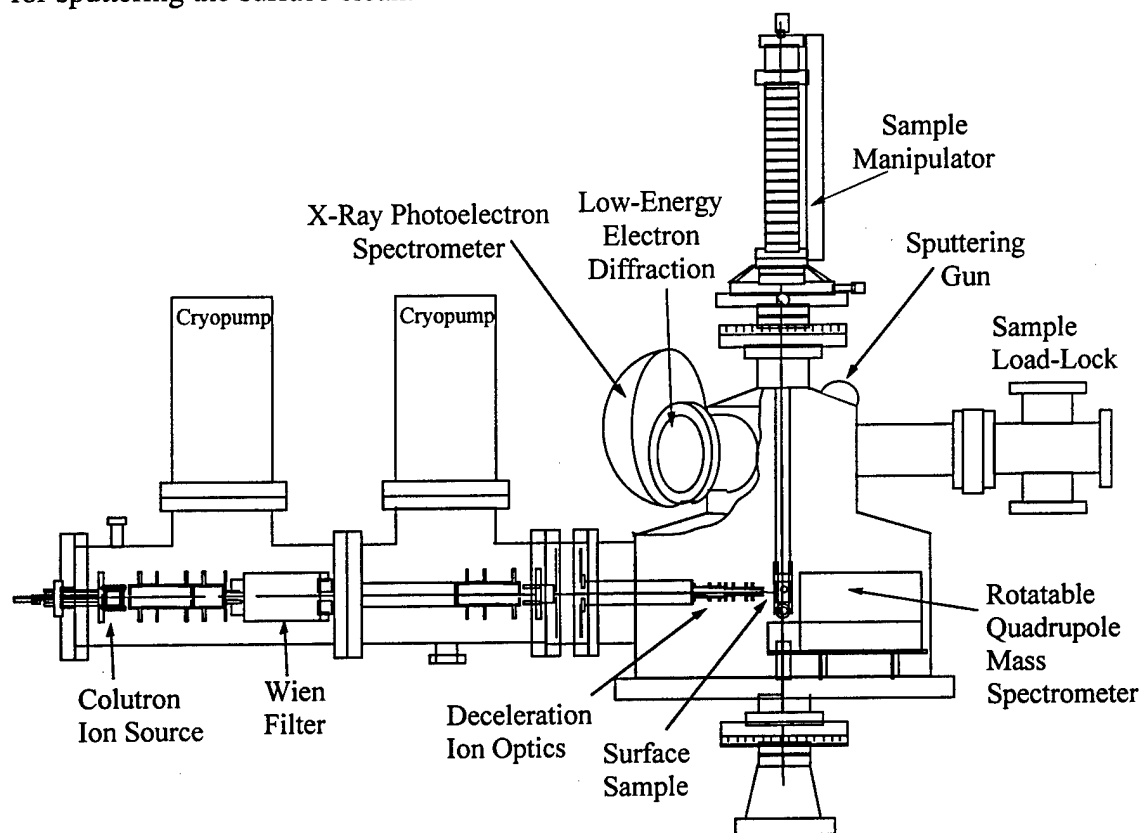


**Figure 1 Atomic Ion/Surface Scattering Apparatus**

Scattering experiments take place in the lower tier of the main chamber. Here a sensitive QMS detector counts individual scattered particles with angle-, energy-, and mass-resolution. Both positive and negative ions are collected with high efficiency.



Furthermore, XPS, Kelvin probe measurements, and temperature-programmed desorption (TPD) are utilized to characterize the surface composition before and after ion beam exposure. In this way, surface modifications induced by energetic particle bombardment are detected.

Two computer data acquisition systems control all the ion optics' potentials and monitor the spectrometer signals. At a series of collision energies, the scattered energy distribution for each product channel is recorded. The angle of incidence and the detection angle are independently varied.

A second differentially pumped, UHV chamber has been implemented for scattering state-selected molecular ions on well-characterized surfaces (Fig. 2). Details are published elsewhere, and only a brief description will be provided here.<sup>3</sup> The gas of interest is introduced via a supersonic expansion through a pulsed valve. Two stages of differential pumping and a cryopump positioned at the throat of the molecular beam eliminate any pressure rise in the main chamber during operation.

The frequency-doubled output of a Nd:YAG-pumped dye laser is tuned to a resonant transition for the molecule. REMPI occurs at the point where the focused 6 ns laser pulse intersects the molecular beam axis. The resulting pulse of ions is extracted with DC electrostatic fields. The ions are accelerated to 200 eV, mass-selected by a Wien filter, decelerated to the final beam energy, and collide with the surface at normal incidence. The surface sample is resistively heated and is cooled with liquid nitrogen. Low Energy Electron Diffraction (LEED) and Auger Electron Spectroscopy (AES) provide a measure of the surface order and cleanliness, respectively. A quadrupole mass spectrometer is employed in the recording of temperature programmed desorption (TPD) spectra.

Both incident and scattered ions are detected with a novel two-dimensional velocity image detector.<sup>4</sup> The ions normally drift field-free on their path towards and

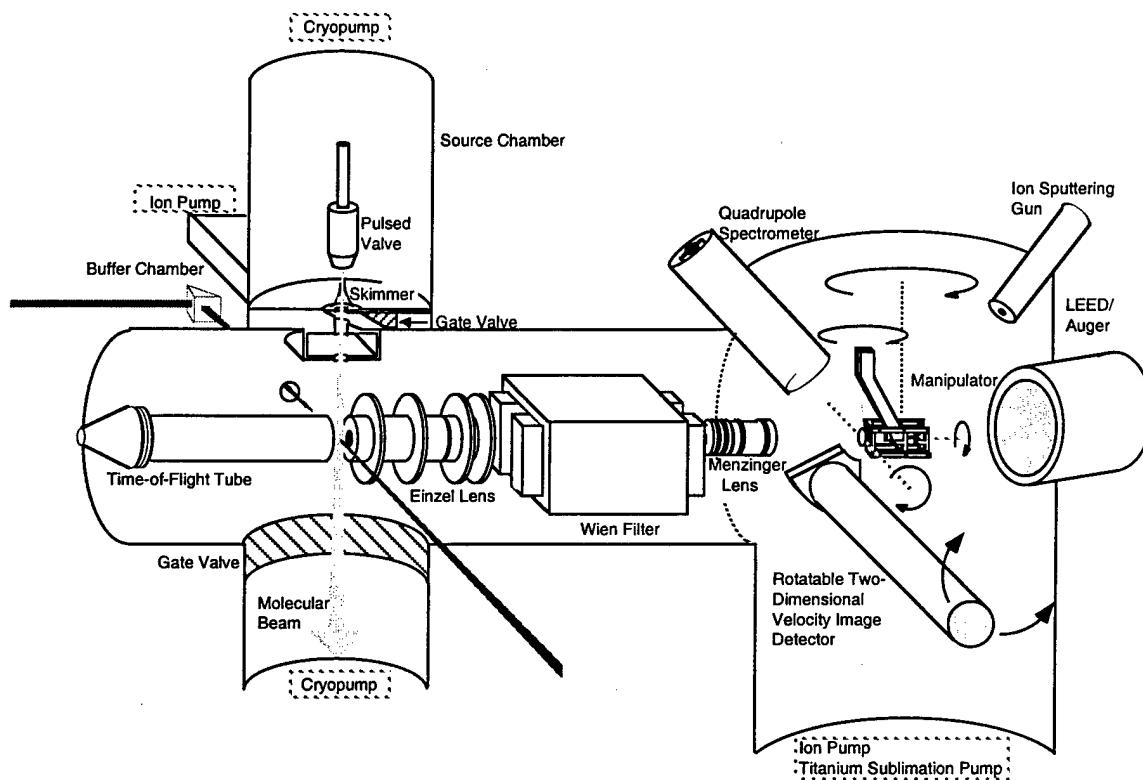


**Figure 2**      **Experimental Apparatus for Scattering State-Selected Molecular Ions**

away from the surface; however, at a pre-determined delay after the laser pulse, a high voltage pulse on a repeller plate redirects the ions down a flight tube into a pair of microchannel plates (MCP). The MCP is gated to allow for mass discrimination in the time-of-flight tube. Recent improvements in our two-dimensional velocity image detector provide us with mass resolution of  $m/\Delta m > 30$ .<sup>5</sup> Each ion striking the MCP delivers  $10^6$  electrons to a phosphor screen, providing a two-dimensional image of the spatial distribution the ions had at the time of the repeller pulse. A charge-coupled device (CCD) camera records the screen's image; a computer then digitizes, averages, analyzes, and stores the camera frames. As a result, ions are detected with single-particle efficiency and are resolved simultaneously according to their charge, mass, velocity, and

scattering angle. In addition, because the same detector counts the number of ions incident and scattered from the surface, absolute survival probabilities and product yields can be reported.

## 4. Results and Discussion

### 4.1. Energy Coupling in Hypervelocity Gas/Surface Collisions

Satellite drag is directly proportional to the momentum that impinging particles (atoms/molecules/ions) transfer to an orbiting spacecraft along the orbital velocity direction. Predictive models currently underestimate satellite drag, in part because they are missing an accurate description of the particle/surface scattering dynamics. The following study examines momentum transfer for a prototypical ion/surface scattering system.

Hyperthermal energy  $\text{Ne}^+$  was targeted at a  $\text{Si}(001)$  surface under conditions where the incident angle and collision energy were systematically varied. The scattered ions were collected with angular-, mass-, and energy-resolution. Figure 3 shows the probability density of  $\text{Ne}^+$  scattering at a particular final angle while retaining a particular fraction of its initial energy.<sup>6</sup>

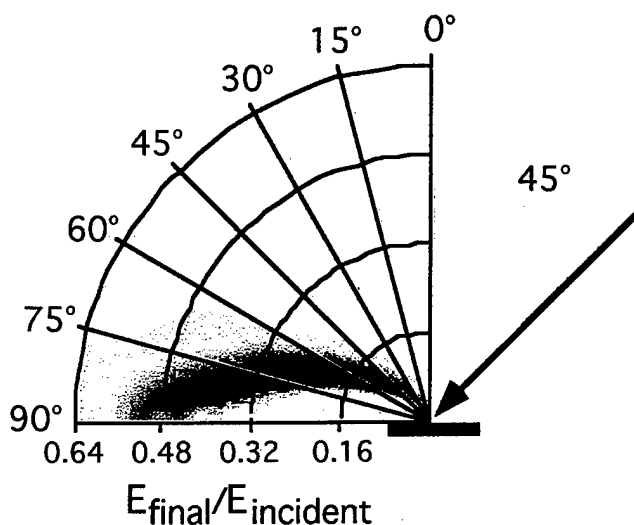


**Figure 3** Angle-Resolved Relative Energy Distribution of 70 eV  $\text{Ne}^+$  /  $\text{Si}(001)$

Figure 3 demonstrates the strong correlation between final scattering angle and final kinetic energy. This scattering behavior is reminiscent of gas-phase collision dynamics, where forward scattering results in minimal energy transfer, and backscattering leads to relatively large amounts of energy transferred. In the binary collision model, the gas-surface collision is represented as a  $\text{Ne}^+$  ion striking a single silicon atom. This approximation of the gas/surface collision is valid in the impulsive limit where short-range repulsive interactions dominate, and where the motion of the  $\text{Ne}^+$  projectile is fast relative to the motion of the recoiling surface atom.

Two approaches were taken to simulate the data. In the first, a phenomenological model was developed that used only a few adjustable parameters to fit over a thousand data points. The second approach involved running classical trajectory calculations on a model system in which  $\text{Ne}^+$  interacted with a slab of coupled silicon atoms. The latter calculations are still in progress.

The phenomenological model incorporated: (i) the elastic energy transfer associated with a single binary collision of  $\text{Ne}^+$  and Si, (ii) the attractive image charge potential that arises from the ion interacting with the dielectric surface, and (iii) the distribution of inelastic energy losses suffered during the collision, and (iv) the instrument response function. Figure 4 compares contour plots of the fitted distributions with that of the experimental data for 70 eV and 120 eV collision energies. The parameters of the fit indicate that  $\text{Ne}^+$  is suffering a significant inelastic energy loss ( $\sim 11$  eV) during a quasi-single binary collision. In fact, the fitted distribution of energy losses matches perfectly with the surface plasmon resonance ( $10.8 \pm 0.2$  eV) of Si(001). This suggests that there exists an efficient plasmon excitation mechanism for  $\text{Ne}^+/\text{Si}(100)$  collisions. At higher collision energies, the model fits the data equally well; the corresponding inelastic energy loss distribution is peaked to slightly higher energies, consistent with the excitation of bulk silicon plasmons. Although multiple collisions of  $\text{Ne}^+$  with the surface are possible, the data are best fit with a quasi single scattering model. It is likely that an ion undergoing multiple surface collisions will be neutralized and not be detected.

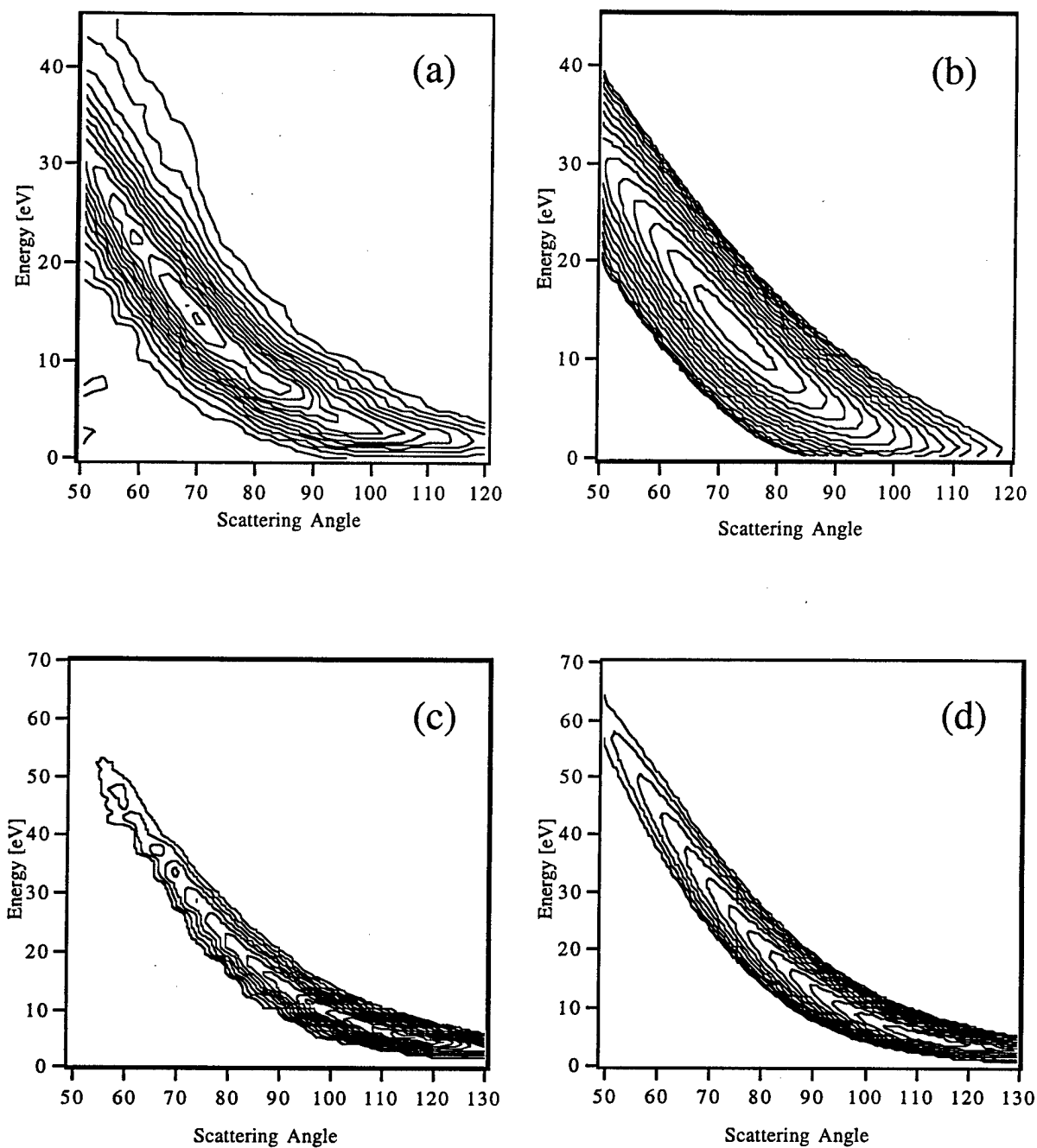


**Figure 4** Comparison of Empirical Fit to  $\text{Ne}^+/\text{Si}(001)$  Scattering Data  
 (a) Experimental data and (b) fit to model for 70 eV  $\text{Ne}^+$  incident at  $45^\circ$ .  
 (a) Experimental data and (b) fit to model for 120 eV  $\text{Ne}^+$  incident at  $45^\circ$ .

## 4.2. Atom Abstraction in the Scattering of State-Selected

### $\text{NO}^+(\text{X}^1\Sigma^+)$ on O/Al(111)

The most abundant molecular ion in LEO is  $\text{NO}^+$ . Little is known about the reactivity of hyperthermal energy  $\text{NO}^+$  with ceramic surfaces. A model surface for scattering studies is  $\text{Al}_2\text{O}_3$ , because it represents a common component in ceramic protective materials. To explore the dynamics of atom-abstraction in hyperthermal ion-surface collisions, state-selected  $\text{NO}^+(\text{X}^1\Sigma^+)$  ions were scattered on O/Al(111), and scattered  $\text{NO}_2^-$  products were detected.<sup>7</sup>

Atom abstraction is an elementary process by which an atom is transferred to or from an incident molecule as the molecule impacts a surface. Gas surface reactions are often assigned to one of two limiting mechanisms: Langmuir-Hinshelwood or Eley-Rideal. In the Eley-Rideal mechanism, an incident gas particle reacts directly with a surface adsorbate, whereas in the Langmuir-Hinshelwood mechanism both reagents thermally equilibrate with the surface prior to reaction.<sup>8</sup> Distinguishing between these two mechanisms is difficult unless one carefully probes the reaction dynamics.

Fig. \_ presents the  $\text{NO}_2^-$  yield as a function of  $\text{NO}^+(\text{X}^1\Sigma^+)$  collision energy for an Al(111) surface dosed with 750 L  $\text{O}_2$ . The  $\text{NO}_2^-$  yield exhibits a threshold energy,  $9 \pm 1$  eV, above which the yield increases linearly with  $\text{NO}^+$  translational energy. The observed threshold is consistent with thermodynamic estimates of the reaction barrier. The  $\text{NO}_2^-$  yield also scales with the total coverage of oxygen on the surface. At the high coverages discussed here, most of the abstracted atoms leading to  $\text{NO}_2^-$  formation originate from islands of chemisorbed oxygen/oxide species on the Al surface.<sup>9</sup>

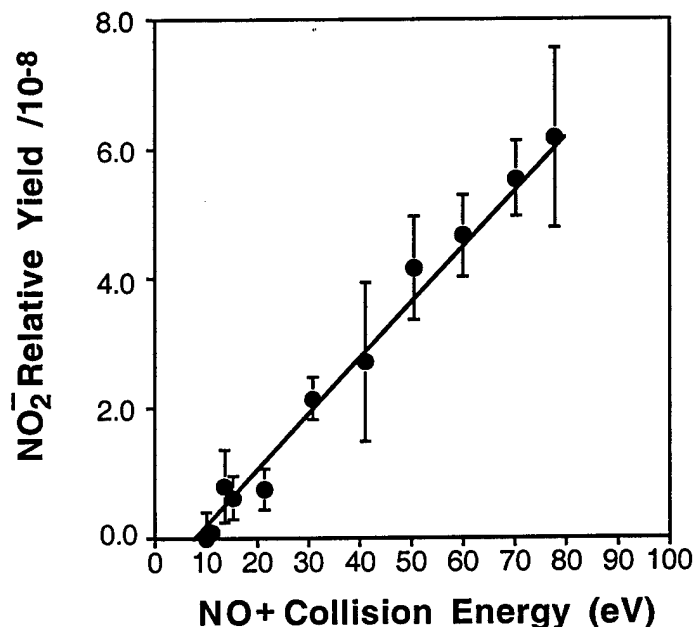


**Figure 5** The collision-energy dependence to  $\text{NO}_2^-$  emergence.

The Al(111) surface was dosed with 750 L  $\text{O}_2$  prior to  $\text{NO}^+$  scattering. The straight line is drawn to guide the eye.

In a Langmuir-Hinshelwood mechanism, the incident NO would thermally accommodate on the surface, diffuse to a chemisorbed oxygen site, react, and desorb as  $\text{NO}_2$ . However, the velocity distribution of scattered  $\text{NO}_2^-$  products is nonthermal and cannot be described by a Maxwell-Boltzmann distribution at the surface temperature (See Fig. 6).<sup>10</sup> Moreover, the mean translational energy of scattered  $\text{NO}_2^-$  increases with  $\text{NO}^+$  collision energy. This correlation implies that the reaction occurs via a direct collision between an incident NO molecule and an adsorbed oxygen atom. The data indicate that neither the incident NO molecule nor the scattered  $\text{NO}_2^-$  product resides on the surface long enough to become thermally accommodated. It is proposed that  $\text{NO}_2^-$  is formed by a three-step mechanism: incident  $\text{NO}^+$  is neutralized close to the surface; nascent NO impacts an adsorbed oxygen atom; and  $\text{O}^-$  is abstracted by NO to form  $\text{NO}_2^-$  via an Eley-

Rideal mechanism. A statistical model is currently being tested to see if it can accurately simulate the experimental data.<sup>11</sup>

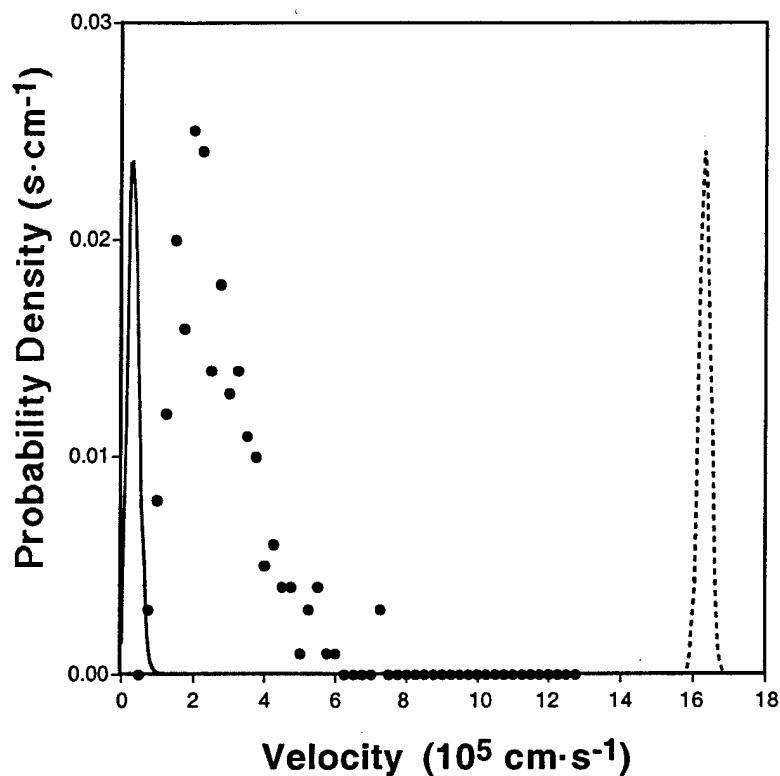


**Figure 6** Velocity distribution of  $\text{NO}_2^-$  products.

40 eV  $\text{NO}^+$  abstracts an oxygen atom from O/Al(111). For comparison, the plot shows the velocity distribution (dashed line) of incident  $\text{NO}^+$ , and the predicted Maxwell-Boltzmann distribution (solid line) if  $\text{NO}_2^-$  were thermally equilibrated with the surface at 300 K.



### 4.3. Growth and Etching of Silicon Oxide Thin Films under $O^+$ Bombardment

The interactions of hyperthermal energy  $O^+$  and  $O_2^+$  with a  $SiO_x$  surface are relevant to the low-earth orbit environment, where energetic oxygen atoms and ions continuously bombard protective coatings, e.g.,  $SiO_2$  on orbiting spacecraft.<sup>12</sup> Furthermore, oxygen plasma processing in the microelectronics industry is frequently used to etch and to deposit oxide films on silicon.<sup>13,14</sup> Despite these important technological applications, a fundamental understanding of the reactivity of hyperthermal energy  $O^+$  and  $O_2^+$  with silicon oxide is lacking. Experimental evidence has been collected to show that 16 – 150 eV  $O^+$  ions directly abstract atomic oxygen from  $SiO_x$  via an ER mechanism, to form scattered  $O_2^-$ .<sup>2</sup>

A silicon wafer, exposed to 60 eV  $O^+$  ions, will develop a thin oxide film, approximately 30 Å thick.<sup>15</sup> Prolonged exposure to the ion beam does not result in a thicker oxide film, because the incident oxygen ions erode the film at the same rate as oxygen deposition. During  $O^+$  ion deposition, both positively and negatively charged scattered products ( $Si^+$ ,  $SiO^+$ ,  $O^-$  and  $O_2^-$ ) were detected.<sup>2</sup> Thus far, the reaction mechanisms leading to  $O^-$ ,  $O_2^-$  and  $SiO^+$  formation have been studied.

Figure 7 shows the  $O_2^-$  yield versus  $O^+$  kinetic energy.<sup>16</sup> Isotopic labeling experiments have helped to define the origin of each oxygen atom in the  $O_2^-$  product. An isotopically pure  $Si^{16}O_x$  film was grown using a mass-selected  $^{16}O^+$  beam. After a  $^{16}O^+$  dose of  $1 \times 10^{16}$  ions/cm<sup>2</sup>, scattering commenced with a mass-selected  $^{18}O^+$  beam. The  $^{34}O_2^-$  product emerges when one oxygen atom from the incident ion beam ( $^{18}O$ ) combines with one oxygen atom from the silicon oxide layer ( $^{16}O$ ). Sputtered  $^{32}O_2^-$  arises when both oxygen atoms originate from the silicon oxide layer ( $^{16}O$ ). The thresholds for  $O_2^-$  abstraction and sputtering occur at  $16 \pm 1$  eV and  $35 \pm 3$  eV, respectively.<sup>16</sup>

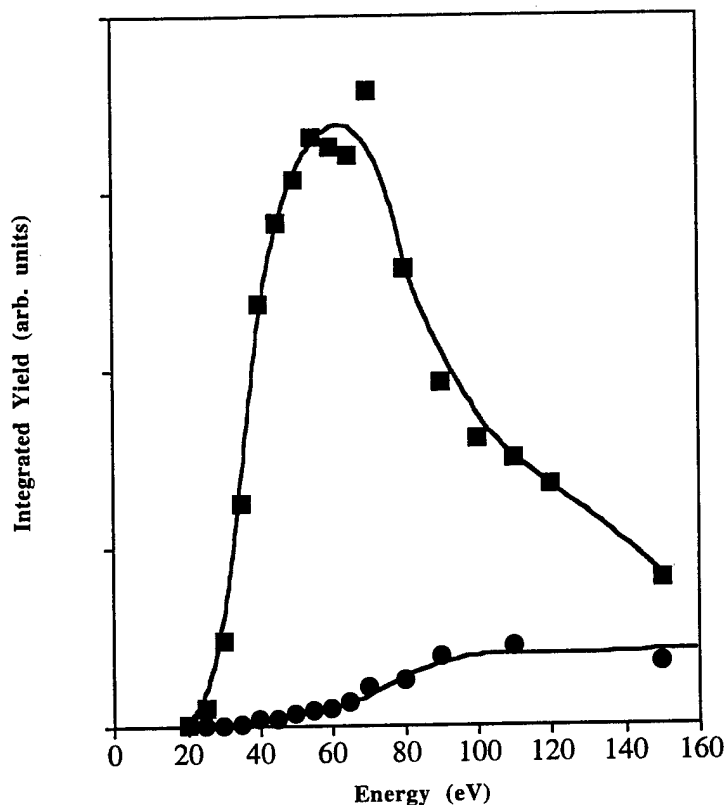


**Figure 7** Yield of  $\text{O}_2^-$  versus incident  $\text{O}^+$  energy.

The squares represent  $^{34}\text{O}_2^-$  products resulting from abstraction. The circles correspond to sputtered  $^{32}\text{O}_2^-$  species.

A variety of mechanisms can describe the association of a projectile and a surface oxygen atom to form  $\text{O}_2^-$ ; yet most can be eliminated in consideration of the experimental evidence. In a Langmuir-Hinshelwood mechanism, an incoming oxygen atom would trap on the surface, become thermally accommodated, diffuse to a neighboring adsorbed oxygen atom, react, and desorb as  $\text{O}_2^-$ . The  $\text{O}_2^-$  product would then be expected to emerge with a translational energy distribution in thermal equilibrium with the surface. Fig. 8 shows that the mean kinetic energy of scattered  $\text{O}_2^-$  correlates strongly with the incident  $\text{O}^+$  kinetic energy. Therefore, the projectile ( $^{18}\text{O}$ ) must be reacting before it has a chance to thermally accommodate with the surface, eliminating a Langmuir-Hinshelwood mechanism. Furthermore, the product  $\text{O}_2^-$  angular distribution shows a strong correlation

with the incident  $O^+$  angle (Fig. 9b). This is direct evidence for an abstraction reaction occurring in a single collision event (Eley-Rideal mechanism), because memory of the incident particle direction would be lost if the  $O^+$  ion encountered multiple bounces on the corrugated surface before abstracting the adsorbed oxygen atom.

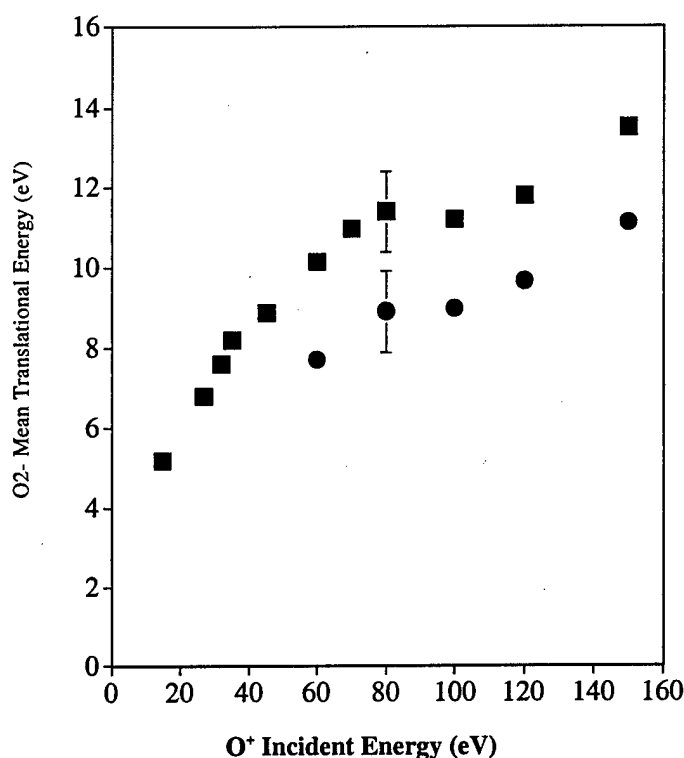


**Figure 8** Mean translational energy of scattered  $O_2^-$  product .

$O^+$  is incident at  $45^\circ$  on an oxidized Si(100) surface. The squares and circles represent  $^{34}O_2^-$  and  $^{32}O_2^-$  products resulting from abstraction and sputtering mechanisms, respectively.

The scattering distribution of  $^{32}O_2^-$  products, shown in Fig. 9a, is qualitatively different than the distribution of  $^{34}O_2^-$  products, shown in Fig. 9b. Although both product channels scatter near the specular angle, the  $^{32}O_2^-$  products appear with less energy and exhibit a smaller correlation between final energy and scattering angle than do the  $^{34}O_2^-$  species. A detailed look at the similarities between the yields and scattering distributions

of  $^{16}\text{O}^-$ ,  $^{18}\text{O}^-$ ,  $^{32}\text{O}_2^-$ , and  $^{34}\text{O}_2^-$  products reveals that  $\text{O}_2^-$  is formed through one of two competing pathways. At low incident  $\text{O}^+$  energies,  $\text{O}_2^-$  is produced exclusively by scattering-mediated abstraction, where an incident O-atom scatters from the lattice and abstracts a surface O-atom on the outbound trajectory. At higher energies, recoil-abstraction is observed, in which a recoiling surface O-atom collides with a neighboring surface O-atom to form  $\text{O}_2^-$ . The two mechanisms are related in that they share a common exit channel involving abstraction of a bound oxygen atom along the exit trajectory.

At  $\text{O}^+$  collision energies above  $\sim 50$  eV, scattered  $\text{SiO}^+$  products are also observed. Isotopic labeling experiments at 70 eV indicate that approximately 1/3 of the  $\text{SiO}^+$  products arise when an incident oxygen atom directly abstracts a silicon atom from the surface. The remaining 2/3 of the  $\text{SiO}^+$  products result from sputtering.

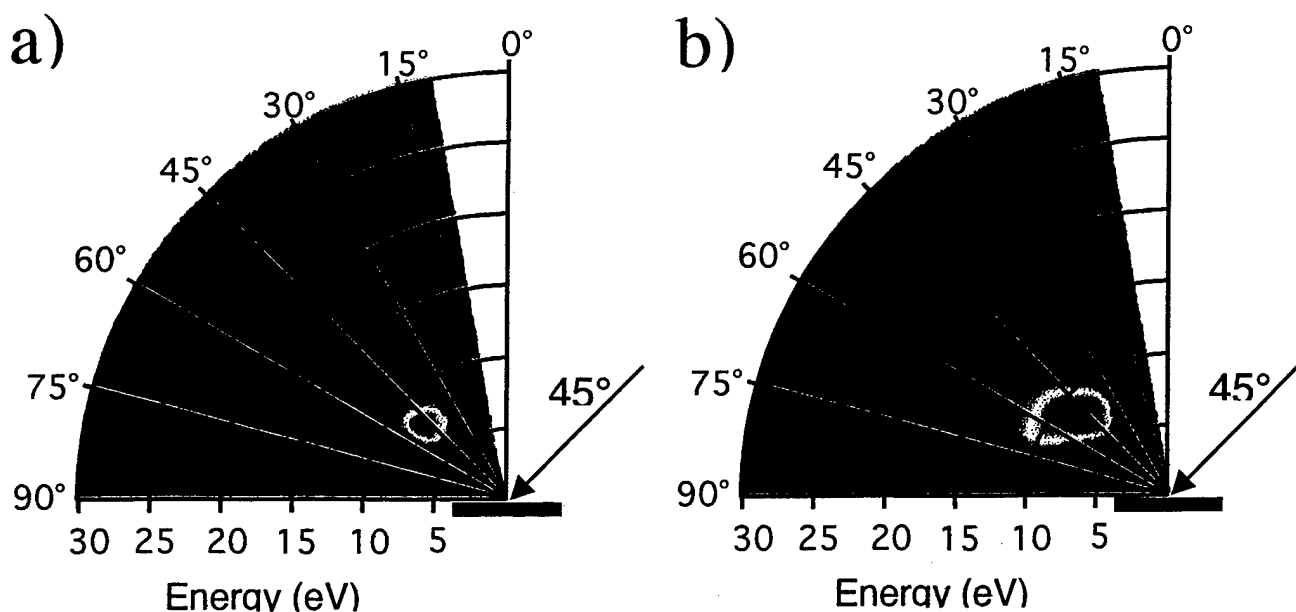


**Figure 9** Angle-Resolved Energy Distributions of  $\text{O}_2^-$  Products.

For 80 eV  $^{18}\text{O}^+$  incident on  $\text{Si}^{16}\text{O}_x$ , the  $\text{O}_2^-$  products are separated into (a) sputtering and (b) abstraction components.

The combination of a mass-filtered ion beam and mass-resolved detection enables the study of ion/surface reactions under high beam exposures where the surface is modified by the bombarding ions. Isotopic labeling techniques have also demonstrated that incident oxygen ions are rapidly incorporated into the silicon oxide film. The cross section, for the incorporation of incident oxygen into the film, is  $2 - 4 \text{ \AA}^2$  for collision energies between 50 and 100 eV.

It is interesting to compare the scattering behavior of  $\text{O}^+$  with that of  $\text{O}_2^+$  on the  $\text{SiO}_x$  surface. Energetic  $\text{O}_2^+$  bombardment of  $\text{SiO}_x$  produces  $\text{O}_2^-$  at lower yields than does  $\text{O}^+$  bombardment. For the  $\text{O}_2^+/\text{SiO}_x$  system,  $\text{O}_2^-$  can emerge from three different mechanisms: direct inelastic scattering of the incident  $\text{O}_2$  molecule, sputtering of adsorbed oxygen, or a substitution reaction with the surface in which one of the incident oxygen atoms in  $\text{O}_2^+$  is replaced with an oxygen atom from the surface. Once again, isotopic labeling experiments are employed to distinguish these three mechanisms, i.e.,  $^{36}\text{O}_2^+$  is scattered on a  $\text{Si}^{16}\text{O}_x$  surface. No evidence for sputtering is observed at collision energies below 60 eV. However, direct inelastic scattering and reactive substitution are competitive, indicating that there is a facile exchange of oxygen atoms at the surface. The angle-resolved energy distribution for reactive substitution shows an energy/angle correlation that is consistent with a direct scattering process. Thus, the substitution reaction must be occurring during a single collision between the incident  $\text{O}_2^+$  molecule and the surface.

## 5. Conclusions

Hyperthermal energy ions can undergo energy transfer, charge transfer, and atom transfer upon impact with a surface. State-of-the-art scattering experiments, combined with theoretical models, have provided detailed information on how these processes occur.

Hyperthermal energy collisions of  $\text{Ne}^+$  with  $\text{Si}(001)$  are well-described by a single impact with a silicon atom, where translational energy is coupled to an electronic excitation in the lattice.<sup>6</sup> The inelasticity of the collision has important implications for the degree of momentum transfer between the particle and the solid. Incorporating these ideas into predictive models for orbital decay may help prolong the lifetime of satellites.

Energetic ions are able surmount chemical barriers that cannot be accessed by thermal molecules. The first demonstration of atom abstraction from an oxide surface was observed in the scattering of  $\text{NO}^+$  on  $\text{O}/\text{Al}(111)$ .<sup>7,10</sup> The production of  $\text{NO}_2^-$  proceeds through an Eley-Rideal mechanism, whereby the incident molecule abstracts an oxygen atom from the surface in a single collision.

Ion beam oxidation of  $\text{Si}(001)$  by 15 – 150 eV  $\text{O}^+$  ions produces a thin  $\text{SiO}_2$  film, approximately 40 Å thick. Further  $\text{O}^+$  bombardment does not increase the thickness of the film; rather, the  $\text{O}^+$  ions oxidize the surface at a rate equal to the rate at which Si and O are removed from the surface through abstraction and sputtering mechanisms.<sup>2,16</sup> Cross sections for incorporating incident O-atoms into the film indicate facile exchange.

These state-of-the-art studies broaden our fundamental understanding of the many reaction pathways available to hyperthermal energy, gas/surface collisions. Furthermore, they are relevant to the bombardment of a space vehicle's exterior surface by energetic species in the ionosphere. The conclusions from this work enhance our ability to predict the interactions between an orbiting spacecraft and the LEO environment, e.g., vehicle drag, spacecraft charging, oxidation/ablation of exposed surfaces, and the formation of signatures.

## 6. References

---

- <sup>1</sup> D. C. Jacobs, "Dynamics of Hypervelocity Gas/Surface Collisions," in *Chemical Dynamics in Extreme Environments*, edited by R. Dressler, *Advanced Series in Physical Chemistry*, World Scientific Publishers, 349 (2000).
- <sup>2</sup> C. L. Quinteros, T. Tzvetkov, and D. C. Jacobs, (2000) "Eley-Rideal reaction of  $O^+$  with oxidized Si(100)," *Journal of Chemical Physics*, **113**, 5119-5122.
- <sup>3</sup> J. S. Martin, J. N. Greeley, J. R. Morris, B. T. Feranchak, and D. C. Jacobs, "Scattering state-selected  $NO^+$  on GaAs(110): The Effect of Translational and Vibrational Energy on  $NO^-$  and  $O^-$  product formation," *Journal of Chemical Physics*, **100**, 6791 (1994).
- <sup>4</sup> D. Corr and D. C. Jacobs, "An Ion Detector for Imaging Two-Dimensional Velocity Distributions," *Rev. Sci. Instrum.* **63**, 1969 (1992).
- <sup>5</sup> M. Maazouz, J. R. Morris, and D. C. Jacobs, "Ion Imaging in Surface Scattering" in *Imaging in Chemical Dynamics*, edited by A. Suits and R. Continetti, American Chemical Society, 139 (2000).
- <sup>6</sup> C. L. Quinteros, *Ph.D. Dissertation*, University of Notre Dame (2001).
- <sup>7</sup> M. Maazouz, T. L. O. Barstis, P. L. Maazouz, and D. C. Jacobs, "Atom abstraction in the Scattering of state-selected  $NO^+(X^1\Sigma^+)$  on O/Al(111)," *Phys. Rev. Lett.* **84**, 1331 (2000)
- <sup>8</sup> W. H. Weinberg, in *Dynamics of Gas-Surface Interactions*, ed. C. T. Rettner and M.N.R. Ashfold (Royal Society of Chemistry, London, 1991), p. 171.
- <sup>9</sup> H. Brune, J. Wintterlin, J. Trost, G. Ertl, J. Wiechers, R. J. Behm, *J. Chem. Phys.* **99**, 2128 (1993).
- <sup>10</sup> M. Maazouz, C. L. Quinteros, T. Tzvetkov, P. L. Maazouz, X. Qin, T. L. O. Barstis, and D. C. Jacobs, "Reactive Collisions of Hyperthermal Ions with Oxide Surfaces" *Proceedings of the Sixteenth International Conference on the Application of Accelerators in Research and Industry: CAARI (2000)*, in press.
- <sup>11</sup> P. L. Maazouz, M. Maazouz, D. C. Jacobs, *to be submitted*.
- <sup>12</sup> E. Murad, *Annu. Rev. Phys. Chem.* **49**, 73 (1998).
- <sup>13</sup> S. C. Mcnevin, *J. Vac. Sci. Tech. B* **8**, 1185 (1990).
- <sup>14</sup> N. Herbots, O. C. Hellman, P. Ye, X. Wang, and O. Vancauwenberghe, *Low Energy Ion-Surface Interactions*, edited by J. W. Rabalais (John Wiley & Sons, 1994), Chapter 8.
- <sup>15</sup> S. E. Todorov and E. R. Fossum, *J. Vac. Sci. Technol. B* **6**, 466 (1988).

---

<sup>16</sup> C. L. Quinteros, T. Tzvetkov, X. Qin, and D. C. Jacobs "Reactive Scattering of O<sup>+</sup> on oxidized Si(001) "

*Nuclear Instruments and Methods in Physics Research B*, in press (2001).